Manuscript for AIAA Aviation (Aeroacoustics) Conference, June, 2015, Dallas

Investigating the feedback path in a jet-surface resonant interaction

K.B.M.Q. Zaman[1], A. F. Fagan[2], J.E. Bridges[3] and C. A. Brown[4]
NASA Glenn Research Center
Cleveland, OH 44135

Abstract

A resonant interaction between an 8:1 aspect ratio rectangular jet and flat-plates, placed parallel to the jet, is studied experimentally. For certain locations of the plate relative to the jet, the resonance takes place with a loud accompanying tone. The sound pressure level spectra are often marked by multiple peaks. The frequencies of the spectral peaks are studied as a function of the streamwise length of the plate, its relative location to the jet as well as the jet Mach number. It is demonstrated that the tones are not due to a simple feedback between the plate's trailing edge and the nozzle's exit; the leading edge of the plate also comes into play in the frequency selection. With parametric variation, it is found that there is an order in the most energetic spectral peaks; their frequencies cluster in distinct bands. The 'fundamental', i.e., the lowest frequency band is explained by an acoustic feedback involving diffraction at the plate's leading edge.

1. Introduction

Over-the-wing engine design is considered in some newer aircraft concepts that might provide a shielding effect for the jet noise propagated towards the ground. In these concepts rectangular geometries for the jet nozzle are preferred for ease of integration with the airframe and also for possible noise benefit inherent to the non-axisymmetric geometry [1-3]. However, the flow from the nozzle is close to a surface before emanating as a free jet and noise from jet-surface interaction becomes an issue. In 2012 a research program was initiated to investigate this experimentally. Plans were developed for detailed experiments in the Aeroacoustics Propulsion Laboratory (AAPL) of NASA Glenn Research Center (GRC). In support of these plans, and in order to provide a database for an ongoing analytical effort in a timely manner, it was decided that a preliminary experiment be carried out in a relatively smaller facility (referred to as 'CW17') during the Fall of 2012. Hot-wire and Pitot-probe surveys together with limited noise measurements were conducted. A comparison of the results with the analysis was made in [4]; see also [5] for details of the analysis.

[1] Inlet & Nozzle Branch, Aeropropulsion Division.
[2] Optics and Photonics Branch, Communication and Intelligent Systems Division.
[3] Acoustics Branch, Aeropropulsion Division.
[4] Acoustics Branch, Aeropropulsion Division.

During the course of the latter experiments, a resonant interaction was encountered. It occurred for certain ranges of the plate's location relative to the nozzle and at high subsonic Mach numbers. It was accompanied by a loud tone that obviously impacted the radiated noise. An understanding of the resonance was important not only to guide future research but also so that it could be avoided or suppressed in applications.

Thus, while experiments on jet-surface interaction simulating practical flows were conducted in the AAPL [6, 7], the resonance phenomenon was pursued further in the smaller (CW17) facility. The latter study involved the simple geometry of a rectangular flat plate with large width placed on one side of the jet. An 8:1 aspect ratio rectangular nozzle was used and the plate was placed parallel to the major-axis plane. Parametric dependence of the resonance was explored by varying the jet Mach number, the plate's streamwise length as well as its relative locations. Earlier results ruling out structural vibration as source of the resonance and on details of the flow field have been presented in [8]. This conference paper covers subsequent explorations aiming at understanding the feedback process in the resonance. A Journal paper summarizing the entire study is anticipated at a future date.

2. Experimental Facility and Procedure

The 'CW17' open jet facility is used for the study. Compressed air supplied through a 30" diameter plenum chamber exhausts through the nozzle into the ambient of the test chamber. Further description of the facility can be found in earlier papers, e.g., [9]. With a suitable adapter, the same nozzles used in the AAPL can be studied in this facility and vice versa. The 8:1 aspect ratio nozzle, referred to as 'NA8Z' in [10] is used in the experiment. It is one of various nozzles that, in combination with different surfaces, were to be studied in the AAPL experimental program. The design considerations for various rectangular nozzles including this one have been discussed in [10]. Detailed coordinates, suitable for adaptation in numerical simulation, can also be found in [9]. The nozzle exit has dimensions of 5.339"x0.658" and thus an equivalent diameter, D=2.12". Because plates with different lengths are used and since there is an ambiguity whether the equivalent diameter or the long or the short dimension of the nozzle is the appropriate length scale, the results are presented simply in dimensional form with unit of distance in inches. Furthermore, when quoting a dimension in equation form, the notation for inch (") is dropped for brevity.

The experiments are conducted with ½"-thick by 24"-wide aluminum plates having variable length L in the streamwise direction. Figure 1(a) is a photograph of the overall setup for the experiment; a schematic with coordinate system and various dimensions is shown in Fig. 1(b). Plate length was varied in the range 2"<L<16" in increments of ½". For brevity, notations such as '8L' will be used to denote a plate of length L=8". For all data, the plate is placed aligned with the nozzle's long edge, centered in the lateral (y) direction relative to the jet axis, and parallel to the x-y plane. The transverse (z) location of the plate could be varied manually using a heavy duty

'lab-jack' (located between the breadboards marked 6 and 7 in Fig. 1a). The axial (x) location could also be varied manually in coarse steps by sliding the plate assembly on breadboard 7.

The test cell has acoustic linings on the ceiling and upper walls and with proper preparation qualitative noise measurement is possible. For the present study, precise amplitudes of the sound pressure level (SPL) spectra are of little concern and the focus is on parametric dependence of the tone frequency. Microphones (¼", B&K 4135) held fixed on an overhead arm are used for the noise measurements. All data presented in the following pertain to an angular location, θ=60˚, referenced to the jet's downstream axis; (preliminary surveys showed that the tone was detected most prominently around this location). The 60˚ microphone is 50.1" away from the center of the nozzle's exit. Spectral analysis is done over 0-10kHz with a bandwidth of 12.5 Hz. The bandwidth primarily dictates the uncertainty in the measurement of the tone frequency.

A focusing schlieren system is used for flow visualization. The system is based on a lens and grid technique where a source grid is projected onto a retro-reflective screen and imaged onto a cut-off grid creating the schlieren effect; an interested reader may find details in [11]. The light source illuminating the flowfield has 1-microsecond pulse duration. All optical components, as well as the scientific-grade CCD camera are housed in a 23"x17"x10" case (item 10 in Fig. 1a). The case is placed on one side of the jet while the 30" x 24" retro-reflective screen is placed on the other side. The distances of the two items dictate the size of the field of view. The chosen distances, within the constraints of the test chamber, provides a field of view that extends approximately 9" in the streamwise direction. The thickness of the focused field (in y-direction) is estimated to be about 3".

Only cold (unheated) flows are considered in the experiment. A jet Mach number (M_j) range from 0.5 to just over 1.0 was covered. The jet Mach number is calculated from the plenum pressure (p_0) and the ambient pressure (p_a) via the isentropic relation, $M_j = (((p_0 / p_a)^{(\gamma-1)/\gamma} - 1)\frac{2}{\gamma - 1})^{1/2}$, where γ is the ratio of specific heats for air.

3. Results

The dependence of the resonance on various parameters is explored. Key results are presented in the following. Figure 2 shows SPL spectra for varying z-location of plate 8L in a 'water fall' pattern. The spectral traces are staggered by one ordinate division with the scale pertaining to the trace at the bottom. The axial location of the plate's trailing edge (TE) is held constant at x_{TE}=8.5; thus, the leading edge (LE) is at x_{LE}= 0.5. The z-location for each spectral trace is indicated in the figure. Each trace is characterized by multiple peaks. A peak at about 1200Hz

becomes dominant around z= -1.5. This is accompanied by a loud audible tone. With varying z the frequency of the tone varies slightly.

Sample schlieren flow visualization images are shown in Fig. 3 for plate 8L. The data are for M_j =0.96 with x_{TE} =8.5 and shown for four z-locations of the plate. The pictures represent 'instantaneous' snapshots with 1 microsecond exposure. For z= -0.5 and -1.0 (plate close to the jet in (a) and (b)) the resonant tone is either absent or weak and the jet basically hugs the plate surface. At z= -1.35, however, there is a clear tone at 1190 Hz and this is accompanied by an undulating flapping motion of the jet column (Fig. 3c). A rolled up vortical structure is apparent just past the trailing edge. For z= -2.2, on the other hand, the tone has diminished in amplitude and the path of the jet has become relatively straight (Fig. 3d).

From the schlieren data (Fig. 3c), one may get the impression that the resonance under consideration might be akin to classic edgetone phenomenon [12, 13]. Here, the resonance might be occurring due to sound pulses produced during the passage of the vortices over the plate's trailing edge. The sound pulses travel back to the nozzle lip to produce nascent vortices completing the feedback loop. This notion, however, is conflicted with the following data. Figure 4 shows spectral data where the trailing edge of the plate is held fixed (x_{TE} =8.5, z= -1.55) while the plate length L is varied. If the resonance is due simply to a feedback between the plate's TE and the nozzle, one may expect the resonant frequency to remain unchanged. As seen in Fig. 4, the spectral shapes and the frequencies of the peaks vary with varying L.

It is apparent that the leading edge (LE) location also comes into play in determining the various spectral peaks. This is further explored in Fig. 5 where the leading edge is held fixed (x_{LE} =0, z= -1.8) while L is varied. Large changes in the spectral shape are seen. Thus, LE location alone also does not determine the frequency.

While the data shown in Figs. 2, 4 and 5 pertain to a fixed jet Mach number M_j = 0.96, the effect of M_j for the 12L plate with fixed position is shown in Fig. 6. One finds that a sharp spike accompanied by audible tone ensues with increasing Mach number around M_j =0.77, for the given configuration. The resonance persists throughout the transonic regime but abruptly stops around M_j =1.06. Note that besides the dominant peak there are other conspicuous peaks in all the spectra shown in Figs. 2, 4-6. The frequencies of these spectral peaks are discussed shortly.

That the leading edge affects the frequencies of the spectral peaks is demonstrated further by the following tests. Recall that detailed experiments were conducted in the AAPL. The spectral data for a 12" long plate with various locations relative to the same NA8Z nozzle indicated a significant difference. No sharp tones were detected

although the spectra were often marked by multiple peaks. A difference in the configuration between CW17 and AAPL was that there was a fixture attached to the leading edge of the plate in the latter facility. The LE fixture had a cut-out in the middle so that the plate could be traversed all the way to the lip of the nozzle. This LE fixture was brought to CW17 and with the same plate configuration as in the AAPL the noise spectra data were retaken. These data are shown in Fig. 7, with a picture of the setup at the top. It can be seen that with the addition of the fixture, the sharp peak at 1.36 kHz has diminished significantly while some of the lower frequency peaks are all but eliminated. These data corroborate the lack of sharp tones noted in the AAPL, and as with Fig. 4, underscore the influence of the LE in the selection of the resonant frequencies.

It was thought that, perhaps, vortex shedding from the leading edge by the entrained flow caused an unsteadiness ('unsteady breathing' through the gap between the nozzle and the plate) leading to the spectral peaks. In order to test this possibility, data were taken with and without a small gap between the plate's LE and the under-side of the nozzle. These data are shown in Fig. 8. It is clear that the spectra are practically identical with and without the gap. For larger gaps the spectral peak persisted but the frequency shifted slightly (see Fig. 2 for data on z-dependence of the spectra for the 8L plate). This exercise ruled out the 'unsteady breathing' to be the driving mechanism for the resonance under consideration.

However, placing a 'fence' or simply a bar between the plate and the under-side of the nozzle did make significant difference in the spectral peaks. This is shown in Fig. 9. Note that not only the amplitudes but also the frequency of the dominant tone has been affected.

Finally, it was found that wrapping the leading edge with sound absorbing (foam) material diminished the spectral peaks drastically. This is shown in Fig. 10. Whereas in Fig. 10, only part of the plate's LE (spanning the width of the nozzle) was wrapped, wrapping the entire LE was found to make no further change in the spectra.

The spectral data are now analyzed as follows. Each spectrum is scanned for the highest three peaks. Even though in some cases smaller peaks may be at the noise level, a look at the characteristics of these peaks reveals some underlying trends. First, as an example, the amplitudes of the peaks for the case corresponding to Fig. 4, are shown in Fig. 11. The circular (red), diamond (blue) and triangular (green) symbols represent the spectral peaks in order of diminishing amplitudes. (The symbol sizes are chosen to represent the trend; the circles are the largest representing the tallest peaks). Also shown in the figure are OASPL values by the square (black) symbols. The undulations in the amplitudes of the largest peak (circular data) are apparently due to a 'staging' behavior in the frequency variation, as it becomes clear with data shown next.

Variations in the frequencies of the three highest spectral peaks, corresponding to the case of Figs. 4 and 11 (fixed TE, varying L), are shown in Fig. 12. At small values of L, the tallest peak occurs around 800 Hz. The frequency decreases with increasing L until around L=7, the tallest peak shifts to a higher frequency band. With further increase in L, it shifts to a yet higher frequency, followed by some oscillations between the upper two bands. What is remarkable is the fact that all frequency data fall in distinct bands. Ignoring some data scatter, it is amply clear that there is an underlying pattern and all frequency data follow one or another of these bands. Peaks representing each band are usually present in the spectra and one of these becomes dominant depending on the geometric configuration. In Fig. 12, there are three conspicuous bands starting at approximately 800, 1200 and 1600 Hz. From various other datasets presented in the following, it is noted that the frequencies of the three peaks are usually not multiples or submultiples of one another in most cases. On occasions, they seem to be multiples but this appears to be a coincidence. Also shown in Fig. 12 are curves denoted as Eqn.1 that will be explained shortly.

Similar frequency variations for the three highest spectral peaks, corresponding to the data of Fig. 5 (fixed LE, varying L), are shown in Fig. 13. A similar observation can be made as with Fig. 12. Again, the frequency data are not random and fall in one of the multiple bands. The same appears to be true for jet Mach number variation with a fixed plate, as seen from the frequency data in Fig. 14 corresponding to the spectral traces of Fig. 6. Finally, similar frequency data for the effect of z-variation with the 8L plate are shown in Fig. 15. These data correspond to the spectral traces of Fig. 2. A similar observation can be made as with Figs. 12-14.

Possible aerodynamics and acoustic feedback involved in the phenomenon are considered with the sketches in Fig. 16. The fact that both LE and TE of the plate influence the frequency of the spectral peaks led us to first consider the following feedback path. In Fig. 16(a), the likely distribution of the vortices is sketched. Inspection of the schlieren images (Fig. 3c) suggests that there might be more than one vortices over the length of the plate at a given instant. Further schlieren data (not shown here for brevity) indicate that in most cases there are two vortices (i.e., two wavelengths) in the bottom shear layer over the length of the plate. Let us assume that there are n number of such vortices. Each vortex produces a sound pressure pulse upon its passage past the TE. Let us also assume that the feedback takes place via a path underneath the plate. Then, using the notations in Fig. 16(a), the total period of the feedback process can be written as the sum of vortex passage time over the distance x_{TE}/n and the acoustic feedback time over the distance $L+s$. Assuming a vortex convection velocity equal to $0.5cM_j$, where c is the speed of sound in the ambient, the following equation can be written for the frequency,

$$f = c/(2x_{TE}/nM_j + L + s) \qquad \textbf{(1)}$$

Note that the thickness of the plate has been neglected in determining the paths and also that $L = x_{TE} - x_{LE}$. The predictions from Eqn. 1 have been shown in Figs. 12-15. In Fig. 12, prediction for n=1, 2 and 100 are shown. To avoid clutter prediction only with n=2 are shown in the subsequent figures. It is apparent that the prediction (n=2) approximates the band of frequency data at the bottom of each figure.

Thus, the simple feedback hypothesis considered above reasonably explains the lowest frequency band for any parametric variation. However, the observation made in Fig. 8 conflicts with the assumed feedback via a path underneath the plate. When the gap between the under-side of the nozzle and the plate's LE was closed by touching the two surfaces, (making sure no light passed through the gap), the spectral shape remained practically unchanged. That is, a small gap or no-gap made no difference in the spectra as long as the junction involved hard surfaces. Insertion of sound absorbing material in the same gap, however, suppressed the resonance (Fig. 10). These observations suggested that the feedback may not be via a path under the plate and led to the following thought.

It is possible that diffraction from the LE creates a 'new' source of sound. This is schematically shown in Fig. 16(b). The sound originating from the TE may travel along a path over the surface (dashed wave fronts). The wave fronts are shown relatively packed for clarity but in reality they may be spaced wider (i.e., longer wavelengths). The waves are diffracted at the LE whence new waves (solid fronts) are radiated in all direction. The source at the LE is nearer to the nozzle lip and thus may have a stronger influence in the feedback in the following sense. The waves from the TE will also reach the nozzle lip but those have to travel through regions of flow and thus get distorted before impacting on the nozzle lip. The LE, on the other hand, is near the lip and in a region where there is no significant flow. Thus, the waves from the LE remain spatially coherent and undistorted when impacting on the nozzle lip. This might explain a stronger influence of the LE in the feedback process even though the original source of the sound waves is at the TE. The part of the dashed waves reaching the LE to get diffracted travels through regions of minimal flow (hugging the plate surface and partly through the boundary layer over the plate) and thus are not distorted.

With the scenario described in the previous paragraph, it should be clear that the lengths of the feedback paths (TE to LE traveled by the dashed waves and LE to nozzle lip traveled by the solid waves, and passage over the distance x_{TE} by the vortices) remain the same as before, yielding the same Eqn. 1 for the frequency. It is plausible that a sharp but hard junction near the leading edge, when the gap is closed, would also produce a similar sound source via diffraction, as sketched in Fig. 16(b). It is also plausible why the resonant frequency changed when a bar was attached underneath the nozzle (Fig. 9). The hard junction where diffraction occurred moved downstream shortening the total path and thus leading to a higher resonant frequency. It appears that the diffraction scenario provides a clearer rationale for Eqn. 1.

Two earlier works on trailing edge noise, by Yu & Tam [16] and Olsen & Boldman [17], are worth noting here. Both reported experimental results on the interaction of a rectangular (slot) jet with a flat-plate. Both, however, involved wall-jets (i.e., plate touching the lower lip of the nozzle), a configuration which did not produce significant resonance in the present experiment. Yu & Tam presented shadowgraph data that exhibited large-scale turbulent motion similar to that seen in Figs. 3(a, b). Their data did not seem to exhibit the violent flapping motion seen in Fig. 3(c). Their (averaged) spectral data were also smooth and did not display any peak. In an earlier paper, Tam & Yu (1975) also presented an analysis addressing sound generation by the interaction of the large-scale turbulent structures with the plate. Based on the analysis the authors noted, "…the noise directivity is strongly influenced by diffraction of sound at the leading edge of the plate". The study, however, did not address a resonant condition or the frequencies thereof. Olsen & Boldman, on the other hand, presented narrow-band spectral data. Some of the spectra did exhibit sharp spikes that must have been associated with discrete tones. Unfortunately, the physical configuration of the plate relative to the flow remained from being completely clear. The plate used was large (several feet long by 8 ft wide) but only 1/8" thick. Structural resonance can come into play [8] and it remains unclear if the tones reported have been due to structural modes or fluid dynamic in origin. Other previous works involving jet-airframe interaction noise may be pertinent (e.g., [18], [19]). Diffraction from the TE as well as the LE of the wing may affect spectral content as well as directivity of noise, even for 'under-the-wing' engine configuration. It is interesting that the SPL spectra discussed in [19], in connection with effect of 'gulley height', also involved multiple peaks as often noted in the data discussed here.

Referring back to the discussions of Figs. 12-15, it should be clear that Eqn. 1 (with n=2) predicts the 'fundamental' or the lowest band of frequencies for every parametric variation considered in this study. These parameters include the plate length L for fixed TE or fixed LE location, as well as the jet Mach number M_j and lateral location z of the plate. Note that in Eqn. 1 the effect of z-variation is accounted for by the parameter s (Fig. 16). However, not everything is completely clear. The upper frequency bands in Figs. 12-15 may be considered as 'stages'. In many resonance phenomena, e.g., edgetone or tones from impinging jets, such a staging behavior is observed. The various stages are harmonically related in the sense that, depending on the stage, different but integral number of vortices occurs between the nozzle and the wedge in the case of edgetone or the nozzle and the ground in the case of impinging jet. (The frequencies from one stage to another are usually not exact multiples of each other.) In the present case, if one assumes more than two vortices in the bottom shear layer (n>2) the predicted frequency will be higher. This, however, is not enough to explain the frequencies in the upper stages. Prediction with n=1 and 100 are also shown in Fig. 12. First, it is clear that the curve for n=1 does not agree with any of the data. It is not clear why the 'fundamental' tone of the phenomenon is predicted with n=2; (one may speculate that the nozzle aspect ratio has an influence in determining this factor). Second, one notes that in the limiting case of very large n the first term

in parentheses on the right side of Eqn. 1 becomes zero. This still predicts frequencies lower than the uppermost band in all cases, as illustrated by the curve for $n = 100$ in figure 12. In essence, the mechanism of the upper stages in the frequency data of Figs. 12-15 remains from clearly understood.

4. Conclusions

An experimental study is conducted in order to investigate a resonance phenomenon occurring between a large aspect ratio rectangular jet and a flat plate. The plate is placed parallel to but away from the direct path of the jet. Effect of parametric variation on the phenomenon is studied. With increasing jet velocity the resonance is found to ensue at a high subsonic Mach number. It becomes most prominent around transonic condition and then stops abruptly at low supersonic condition when shocks become prominent in the flow. It occurs for a range of transverse (z) positions of the plate relative to the jet. It disappears when the plate is either too far or too close to the jet. With variation of the plate's z-location the frequency of the resonance varies slightly. The frequency clearly increases with increasing jet Mach number or decreasing streamwise distance of the plate's trailing edge. It is noted that even when there is no audible tone, the noise spectra is marked by conspicuous peaks. It is demonstrated that for a fixed trailing edge location, the frequencies of the spectral peaks also depend on the location of the leading edge. An acoustic feedback process, involving diffraction from the leading edge, is considered and shown to explain the 'fundamental' frequency of the phenomenon.

Acknowledgement:

Supports from the Commercial Supersonic Technology and Advanced Air Transport Technology Projects of NASA's Fundamental Aeronautics Program are gratefully acknowledged.

References:

[1] Balsa, T.F., Gliebe, R.R., Kantola, R.A., Mani, R., Stringas, E.J. and Wang, J.C.F., "High velocity jet noise source location and reduction, Task 2 – theoretical developments and basic experiments", *Report No. FAA-RD-76-79, II*, General Electric Co., Aircraft Engine Group, Cincinnatti, OH, May, 1978.

[2] Massey, K.C., Ahuja, K.K. and Gaeta, R., "Noise scaling for unheated low aspect ratio rectangular jets", *AIAA paper 2004-2946*, 10th AIAA/CEAS Aeroacoustics Conference, Manchester, UK 10-12 May 2004.

[3] Nichols, J.W., Ham, F.E., Lele, S.K. and Moin, P., 2011, "Prediction of supersonic jet noise from complex nozzles", *Center for Turbulence Research Annual Research Briefs*, pp. 3-14.

[4] Afsar, M., Goldstein, M.E. & Leib. S. J., "Prediction of low-frequency trailing edge noise using rapid distortion theory", *14th European Turbulence Conference*, Lyon, France, Sept 1-4, 2013.

[5] Goldstein, M.E., Afsar, M.Z. and Leib, S.J., "Non-homogeneous rapid distortion theory on transversely sheared mean flows", *J. Fluid Mech.*, 2013, (to appear).

[6] Bridges, J.E., Brown, C.A. and Bozak, R.F., 2014, "Experiments on exhaust noise of highly integrated propulsion systems", *AIAA Paper* 2014-2904, 21st AIAA/CEAS Aeroacoustics Conference, Atlanta, GA, 16-20 June.

[7] Brown, C.A. and Wernet, M.P., 2014, "Jet surface interaction test: flow measurements results", *AIAA Paper* 2014-3198, 21st AIAA/CEAS Aeroacoustics Conference, Atlanta, GA, 16-20 June.

[8] Zaman, K.B.M.Q., Fagan, A. F., Clem, M.M., and Brown, C.A., "Resonant Interaction of a Rectangular Jet with a Flat-plate", AIAA Paper 2014-0877, 52nd AIAA Aerospace Sciences Meeting (SciTech2014), January 13-17, 2014, National Harbor, MD.

[9] Zaman, K.B.M.Q., "Flow-field surveys for rectangular nozzles", *NASA TM-2012-217410* (see also *AIAA Paper 2012-0069*), 2012.

[10] Frate, F.C. and Bridges, J.E., "Extensible rectangular nozzle model system", *AIAA Paper 2011-975*, 49th Aerospace Sciences Meeting, Orlando, Fl, 4-7 January, 2011.

[11] Fagan, A.F., L'Esperance, D. and Zaman, K.B.M.Q., "Application of a novel projection focusing schlieren system in NASA test facilities", *AIAA Paper* 2014-2522, 31st AIAA Aerodynamic Measurement Technology and Ground Testing Conference, Atlanta, GA, 16-20 June, 2014.

[12] Brown, G.B., "The vortex motion causing edge tones", *Proc. Phys. Soc.* (London), **49**, pp. 493-507, 1937.

[13] Powell, A., "On the edgetone", *J. Acoust. Soc. of America*, vol. 33, pp. 395-409, 1961.

[14] Tam, C.K.W. and Yu, J.C., "Trailing edge noise", *AIAA Paper 75-489*, 2nd Aero-acoustics conference, Hampton, VA, 1975.

[15] Olsen, W. and Boldman, D., "Trailing edge noise data with comparison to theory", *AIAA Paper 79-1524*, 12th Fluid and Plasma Dynamics Conference, Williamsburg, VA, 1979.

[16] Yu, J.C. and Tam, C.K.W., 1978, "Experimental investigation of trailing edge noise mechanism", *AIAA J.*, vol. 16, no. 10, pp. 1046-1052.

[17] Olsen, W. and Boldman, D., 1979, "Trailing edge noise data with comparison to theory", *AIAA Paper 79-1524*, 12th Fluid and Plasma Dynamics Conference, Williamsburg, VA, 23-25 July.

[18]Miller, W.R., 1983, "Flight effects for jet-airframe interaction noise", AIAA Paper-83-0784, 8th AIAA Aeroacoustics Conference, Atlanta, Georgia, 11-13 April.

[19] Mengle, V.G., 2011, "The effect of nozzle-to-wing gulley height on jet flow attachment to the wing and jet-flap interaction noise", *AIAA Paper 2011-2705*, 17th AIAA/CEAS Aeroacoustics Conference, Portland, Oregon, 5-8 June.

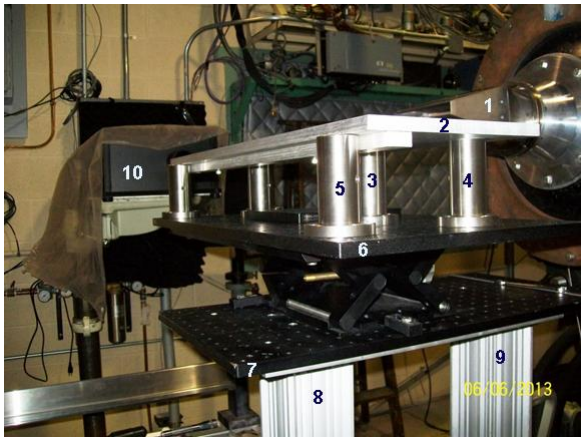

(a)

Fig. 1(a)

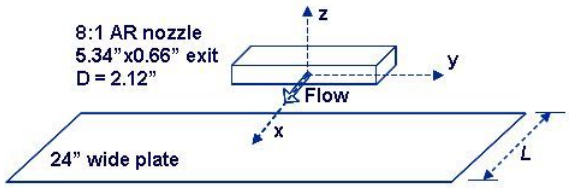

(b)

Fig. 1 Experimental facility. (a) setup with marked components. 1: Nozzle; 2: plate; 3-5: mounting posts; 6,7: breadboards; 8,9: supports; 10: focused schlieren apparatus. (b) schematic of setup with coordinates. Length dimensions in all following figures are in inches.

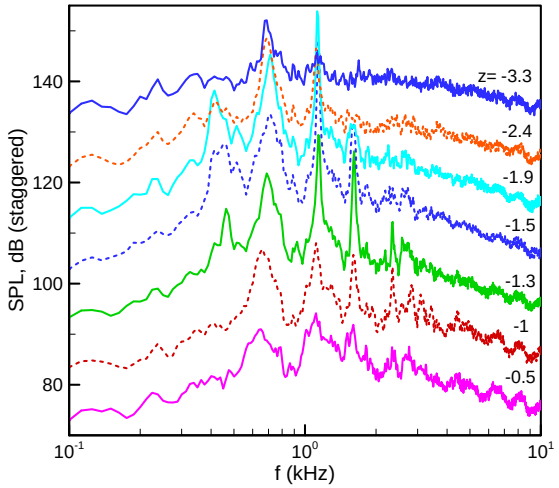

Fig. 2 SPL spectra for varying z-location of plate $8L$; x_{TE} = 8.5, M_j =0.96. Ordinate pertains to trace at bottom, others staggered successively by 10 dB.

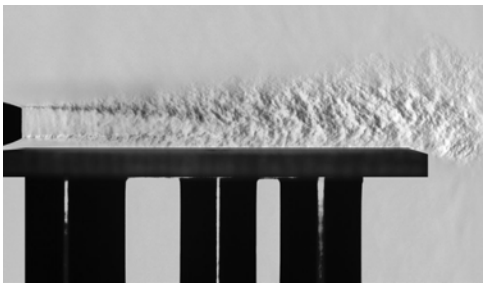

Fig. 3(a)

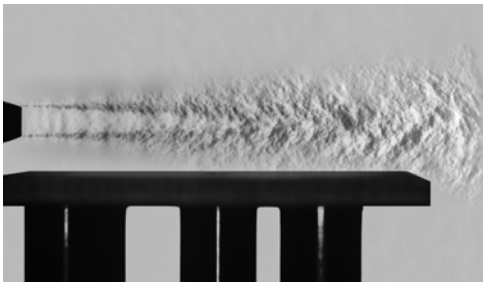

Fig. 3(b)

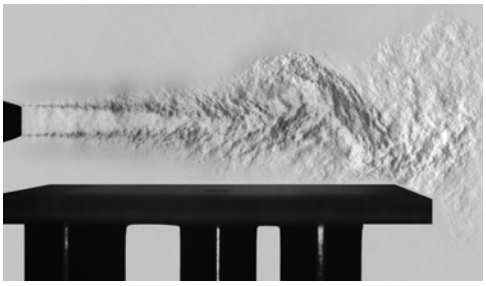

Fig. 3(c)

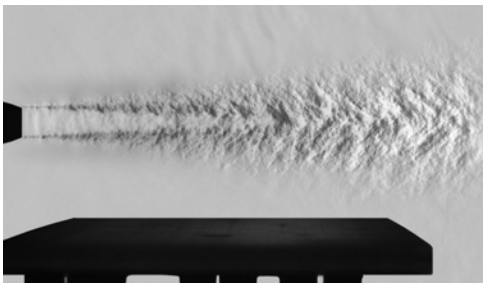

Fig. 3(d)

Fig. 3 Schlieren images of flowfield for varying z-location of plate $8L$; x_{TE} =8.5, M_j = 0.96. (a) z= -0.5, (b) z= -1.0, (c) z= -1.35 and (d) z= -2.2.

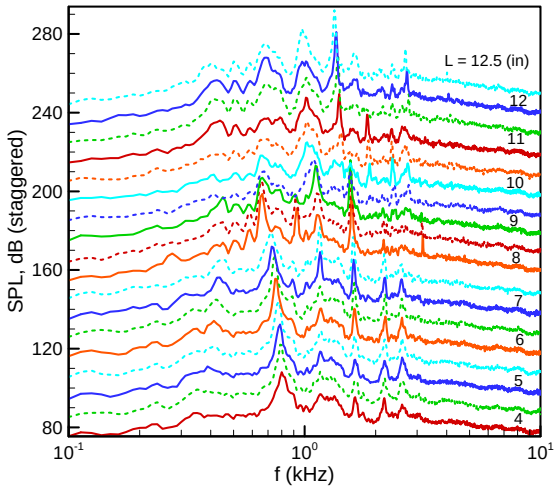

Fig. 4 SPL spectra for fixed TE location of plate (x_{TE} =8.5 and z= -1.55) but varying L (hence varying LE location, x_{LE}); M_j= 0.96. Traces are staggered in same manner as in Fig. 2.

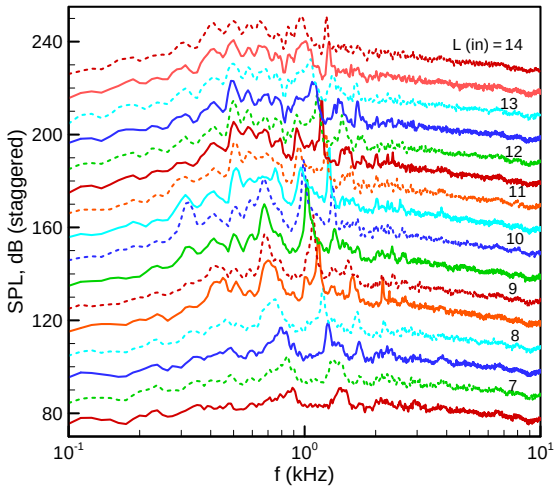

Fig. 5 SPL spectra for fixed LE location of plate (x_{LE} =0, z=-1.80) but varying L (hence varying x_{TE}); M_j= 0.96. Traces are staggered in same manner as in Fig. 2.

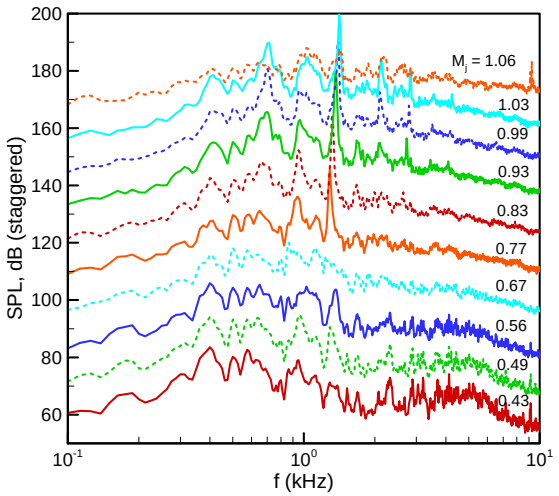

Fig. 6 SPL spectra for varying M_j with plate 12L; x_{TE} =8.5, z= -1.5. Traces are staggered in same manner as in Fig. 2.

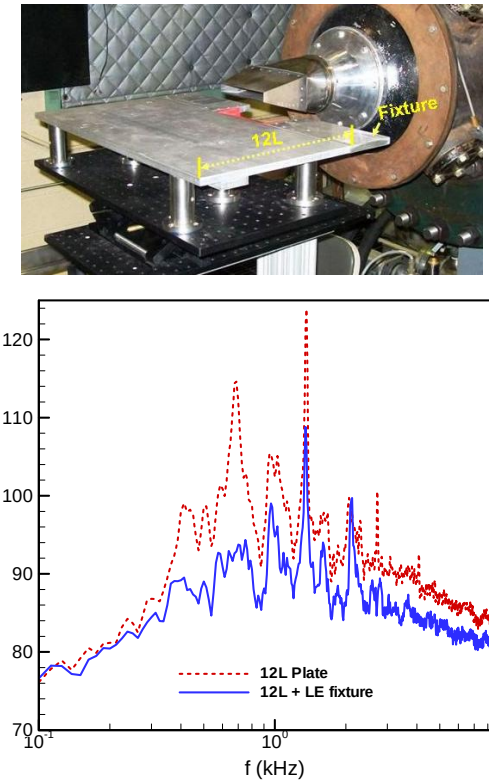

Fig. 7 Effect of attaching a leading edge fixture to plate 12L; x_{TE} =8.5 and z= -1.53; M_j =0.96.

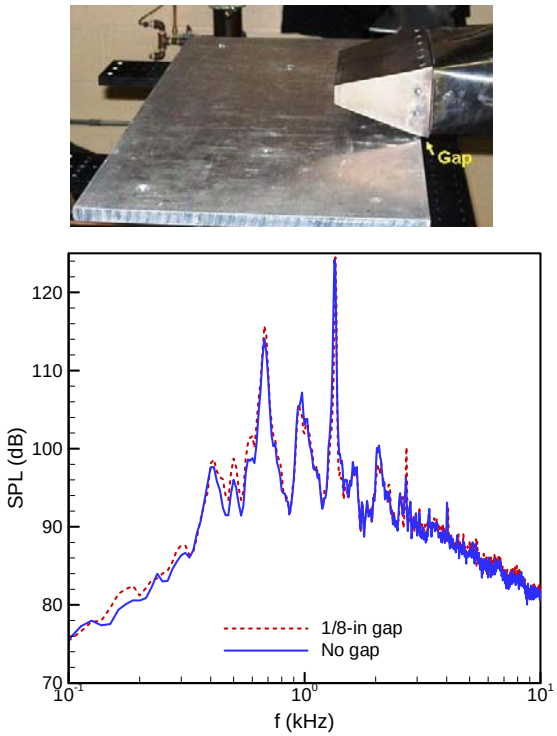

Fig. 8 SPL spectra with and without a 1/8" gap between the plate and the under-side of the nozzle. Plate 12*L* with x_{TE} =8.5, M_j =0.96; dotted line: *z*= -1.53, solid line: *z*= -1.40.

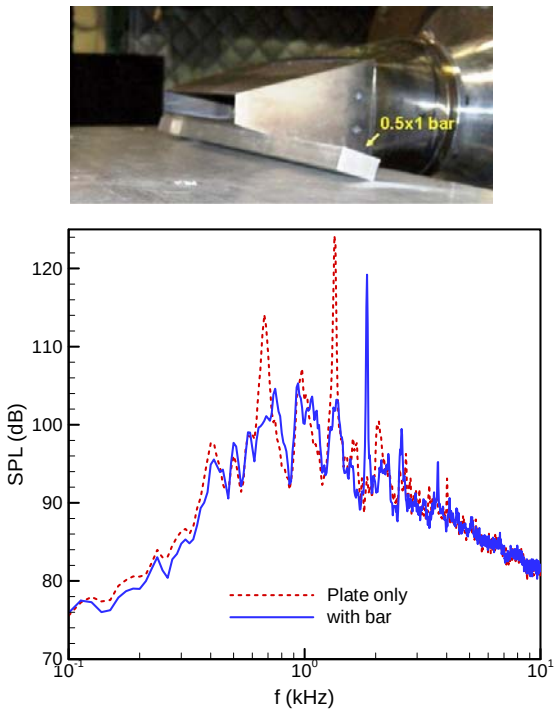

Fig. 9 Effect of a 0.5"x1" bar attached to the under-side of the nozzle; plate 12*L* with x_{TE} =8.5 and *z*= -1.53 at M_j =0.96.

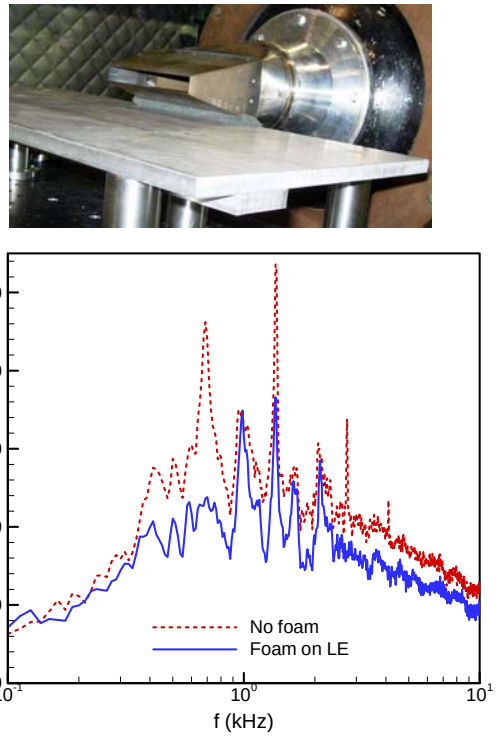

Fig. 10 Effect of placing sound absorbing material near LE; plate 12*L* with x_{TE} =8.5 and *z*= -1.53 at M_j =0.96.

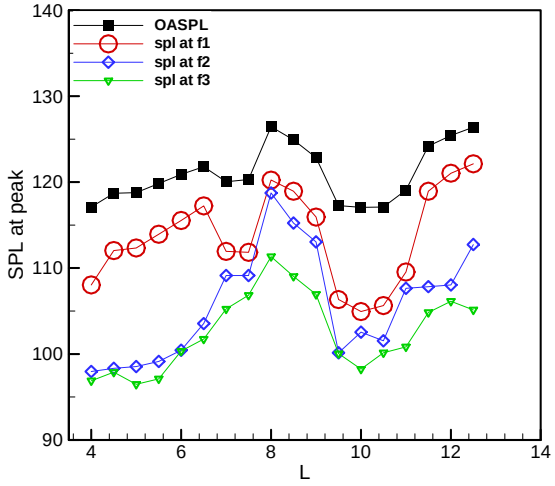

Fig. 11 Amplitudes of three highest peaks in spectra shown in Fig. 4; varying *L* with fixed x_{TE} =8.5, z= -1.55 at M_j= 0.96.

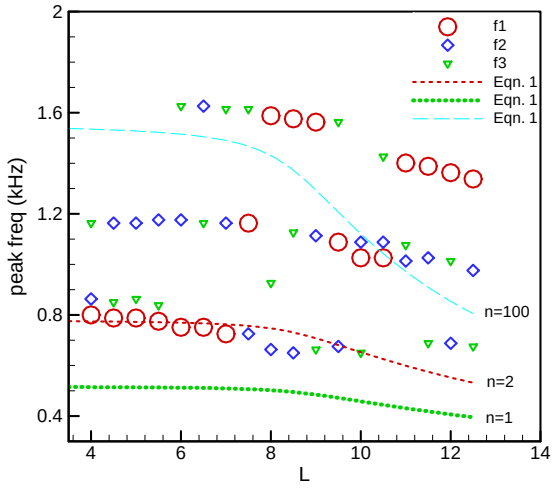

Fig. 12 Frequencies of three highest peaks in spectra of Fig. 4. Varying L with fixed x_{TE} =8.5, z= -1.55 at M_j= 0.96. f1, f2 and f3 denote three peaks in order of deceasing amplitude. Lines for Eqn.1 (see text).

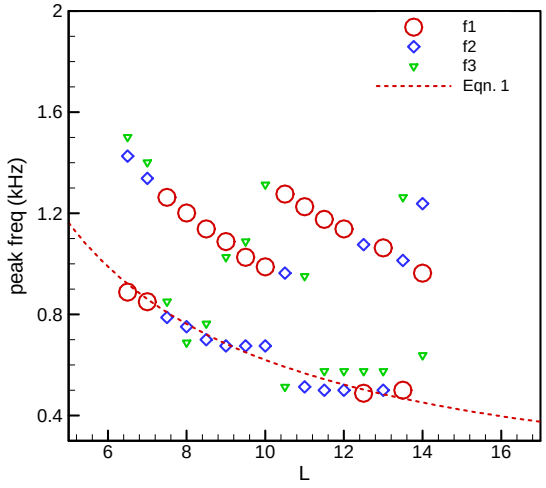

Fig. 13 Frequencies of three highest peaks in spectra of Fig. 5; fixed LE of plate (x_{LE} =0 and z= -1.80) but varying L (hence varying x_{TE}).

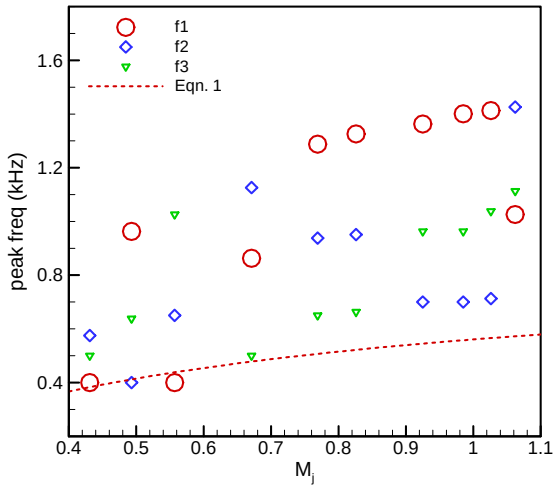

Fig. 14 Frequencies of three highest peaks in spectra of Fig. 6; varying M_j for plate 12L, x_{TE} =8.5, z= -1.5.

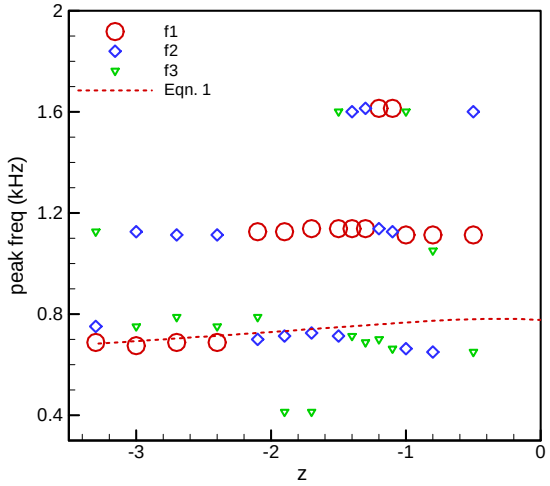

Fig. 15 Frequencies of three highest peaks in spectra for varying z with plate 8L (Fig. 2); x_{TE}=8.5, M_j= 0.96.

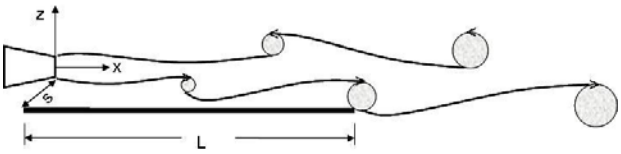

Fig 16(a)

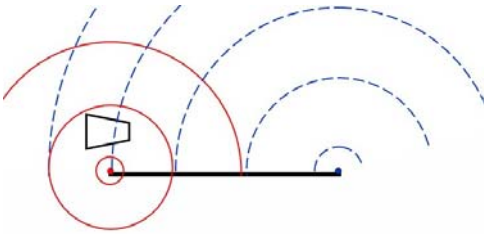

Fig. 16(b)

Fig. 16 Schematics of flow and acoustic diffraction. (a) Likely distribution of vortices in flow, (b) acoustic waves and diffraction from LE.